SCIENCE CHINA
Life Sciences

• RESEARCH PAPER •

December 2014 Vol.57 No.12: 1213–1217
doi: 10.1007/s11427-014-4732-0

# Morphological changes in Schlemm's canal in treated and newly diagnosed untreated glaucomatous eyes

SHI GuoHua[1†], FU LingLing[2†], LI XiQi[1], JIANG ChunHui[3] & ZHANG YuDong[1*]

[1]*Key Laboratory on Adaptive Optics, Institute of Optics and Electronics, Chinese Academy of Sciences, Chengdu 610209, China;*
[2]*Karamay Central Hospital, Karamay 834000, China;*
[3]*Department of Ophthalmology and Vision Science, Eye & ENT, Fudan University, Shanghai 200031, China*

Received March 1, 2014; accepted July 16, 2014; published online September 12, 2014

A custom built 1310 nm center wavelength swept source optical coherence tomography instrument was used to measure morphological changes in treated and newly diagnosed untreated glaucomatous human Schlemm's canal (SC). Thirty-seven primary open-angle glaucoma patients were divided into two groups depending on the patients having been treated or not. The statistical results showed that there were significant differences between the treated and untreated groups' SC areas (treated, 7935.6875±680.003 μm$^2$; untreated, 3890.71875±871.49844 μm$^2$; $P$<0.001), the circumferences (treated, 580.37891±44.96529 μm; untreated, 381.9026±41.22123 μm; $P$<0.001), and the long diameters (treated, 272.87806±25.7254 μm; untreated, 185.24047± 19.72786 μm; $P$<0.001). We hypothesize that, after drug treatment, the SC will expand and the morphometric values especially the areas will become larger, thus helping to reduce intraocular pressure.

**ophthalmology, glaucomatous, Schlemm's canal, morphometry**

**Citation:** Shi GH, Fu LL, Li XQ, Jiang CH, Zhang YD. Morphological changes in Schlemm's canal in treated and newly diagnosed untreated glaucomatous eyes. Sci China Life Sci, 2014, 57: 1213−1217, doi: 10.1007/s11427-014-4732-0

The World Health Organization predicts that 44.7 million people will suffer from primary open-angle glaucoma (POAG) [1]. Abnormally high intraocular pressure (IOP) is related to the development of glaucoma [2,3]. Comparative anatomy results suggest that the Schlemm's canal (SC), which connects the trabecular meshwork and collector canals, is a possible resistance point of aqueous humor outflow in primary open angle glaucomatous eyes. This might explain the approximately 50% decrease of aqueous outflow facility in these patients [4]. The collapse of the SC at higher IOP might be a cause of POAG [5,6]. Therefore, measuring the SC morphometric values quantitatively could provide important information for glaucoma diagnosis and treatment. However, the required resolution is in ten micrometers range. Previous studies were therefore limited to histologic sections of animal eyes [4–6].

With increased revolution in frame rate and sensitivity, in the last few years, optical coherence tomography has been successfully used for SC imaging *in vivo* [7−10]. Kagemann et al. [7] measured the size of SC in one glaucoma patient using 870 nm spectral domain optical coherence tomography (SD-OCT). SC morphometric values of 50 POAG patients were measured by swept source optical coherence tomography (SS-OCT) [8]. Consistent with the *in vitro* studies, the POAG eyes had significantly smaller SC areas compared with those of normal eyes [9]. In normal eyes, age and gender related SC areas have also been determined [10]. Further studies will suggest more uses for SS-OCT in this field. The comparison of different drug treatments in patients with POAG has previously been evaluated by the decrease of IOP [11,12]. Recent *ex vivo* studies show that IOP

†Contributed equally to this work
*Corresponding author (email: ydzhang@ioe.ac.cn)

is also related to SC morphology [13]. Therefore, although the SC may not be a criterion for POAG, it may be used to demonstrate if the SC morphology changes with drug treatment. Thus, it could provide a new approach to drug efficacy evaluation.

In this report, a custom built 1310 nm SS-OCT instrument was designed to demonstrate that SC morphology changes with drug treatment. High speed, high resolution imaging of the ocular anterior segment was achieved *in vivo*, and statistical analysis based on the high resolution SC image was used to verify if the SC morphology was related to drug treatment.

## 1 Materials and methods

### 1.1 Swept source optical coherence tomography system

As shown in Figure 1A and B, light from the swept source is divided by a fiber coupler to the Mach-Zehnder interferometer (5% optical power) and the Michelson interferometer (95% optical power). The interference signal is received by the Michelson interferometer [9]. After calibrating the wave number of the interference signal by the Mach-Zehnder interferometer (INT-MZI-1300, Thorlabs, Newton, NJ 07860, USA), the actual axial resolution was 8.03 μm in the air, and 6 μm in an aqueous solution, measured by assuming the refractive index of water as 1.34. By using the GPU (Graphic Processing Unit) to process the data [14], the system frame rate was 22.5 fps in real time. A 660 nm laser diode functioned as the aiming laser.

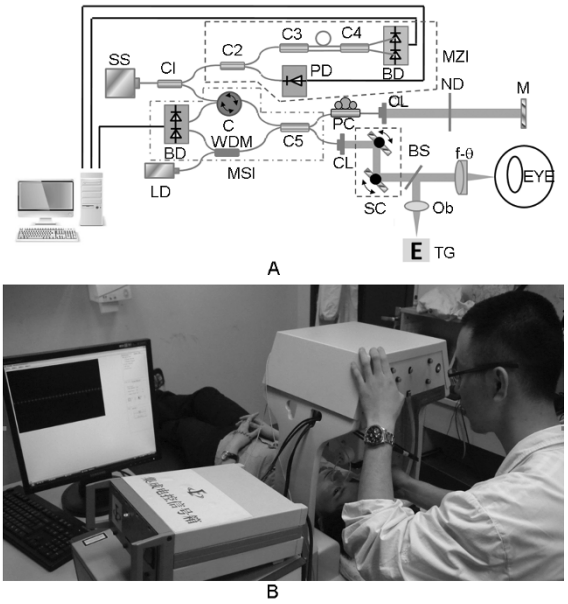


**Figure 1** The custom built SS-OCT system. A, Schematic of SS-OCT system. B, A picture of the SS-OCT system during measurements. SS, swept laser source; C1, fiber coupler (5/95); C2–C5, fiber coupler (50/50); BD, balance detector; PD, photo diode; LD, laser diode; WDM, wavelength division multiplexer; C, circulator; PC, polarization controller; CL, collimator; ND, neutral density filters; M, mirror; SC, x-y scanner; Ob, objective; Bs, beam splitter; f-θ, f-θ scanner lens; TG, target; MZI, Mach-Zehnder interferometer; MSI, Michelson interferometer.

A gantry structure was adapted to allow the subject to lie down during imaging, and positioned each individual subject approximately the same incidence beam angle. To ensure the scanning plane (B-scan) was orthogonal to the SC orientation, a three-dimensional electric translation stage, which could be controlled manually by a frontal control panel, was mounted on a sample arm to adjust the imaging location and focusing position. Table 1 shows the detailed specifications of this SS-OCT system.

### 1.2 Subjects

All subjects were recruited from POAG patients who visited the Eye Ear Nose and Throat Hospital (Fudan University, Shanghai, China). The study was conducted in accordance with the tenets of Declaration of Helsinki, and approved by the Ethics Committee of the Eye Ear Nose and Throat Hospital, Fudan University. Each subject has signed an informed consent agreement. Three common drugs, including timolol, latanoprost and dorzolamide, were used to treat the patients. Timolol and latanoprost can reduce the production of aqueous humor, while dorzolamide improves the outflow of aqueous humor. Because of the limitations of ethics approval requirements, we compared the morphological alterations between treated and untreated glaucomatous human SC, but an efficacy evaluation of different drug treatments was not done. The incident light power (<1.5 mW) of the eye was lower than the maximum allowable exposure, which was safe for the retina. Before the experiments, every patient underwent a complete ophthalmic examination, including IOP determinations (Goldman T900, HAAG-STREIT Diagnostics, Koeniz, Switzerland) and visual field examinations (VF, Humphrey, Kalamazoo Township, MI 49048, USA). Subjects were divided into two groups as follows: the untreated group, with newly diagnosed, untreated POAG patients, and treated group, with patients whose conditions were controlled.

**Table 1** SS-OCT specifications

| System parameter | Performance |
|---|---|
| Center wave length | 1310 nm |
| 3 dB bandwidth | 110 nm |
| Aiming laser | 660 nm |
| Axial resolution | 8.03 μm in the air, 6 μm in aqueous solution |
| A scan rate | 20 kHz |
| Cross-section image format | 800 A-lines×512 pixel |
| Frame rate | 22.5 fps |
| Scan range | Depth: 2.97 mm in the air<br>Transverse: 4.8 mm in the air for 800 A-lines |
| Pixel axial resolution | depth：5.76 μm in the air; 4.3 μm in aqueous solution<br>transverse: 6 μm in the air |
| Power on eye | <1.5 mW |

All patients in the POAG group were bilateral, and a total of 37 participants were involved in the study, 19 in the treated group including 12 men (63%) and 7 (37%) women, from 20 to 74 years of age (average age, 53.3±18.3 years). The IOPs ranged from 12 to 19 mmHg (average, 15.5±1.8 mmHg). The untreated group included 18 patients, 8 men (44%) and 10 (56%) women, from 19 to 77 years of age (average, 49.6±18.5 years), with IOPs from 21 to 29 mmHg (average, 23.6±2.1 mmHg). There was no significant difference in the distribution of age ($P$=0.47) and gender ($P$=0.28) between these two groups. The IOPs of the untreated group were higher than those of the control group.

### 1.3 Quantitative analysis

The cross-sectional images of the anterior chamber angle were taken with our SS-OCT system, including the cornea, iris, scleral spur, trabecular meshwork, and the SC, which is shown in Figure 2A. While performing the measurements, we manually magnified in image and designated the area of the SC. The diameter was then measured by the farthest distance of the two pixels, and the circumference was determined by taking the sum of the distances. The area was obtained by the polygonal area formula as shown in eq. (1),

$$S_{\Omega} = \frac{1}{2}\sum_{i=1}^{M}(x_i \times y_{i+1} - x_{i+1} \times y_i)d_x d_y, \quad (1)$$

where $x_i$ and $y_i$ were the pixels' coordinates, $d_x$ and $d_y$ were the lengths that each pixel represented in transverse and axial planes. Note that, $y_i$ was the pixel axial resolution in aqueous solution, which was 4.3 μm.

Figure 2B is an image from a 45-year-old female patient whose condition was controlled by drugs. Figure 2C is an image from a 47-year-old female patient who had just been diagnosed with POAG. The morphological differences of the SCs between treated and untreated eyes can be observed from the images, and the detailed analysis is discussed below.

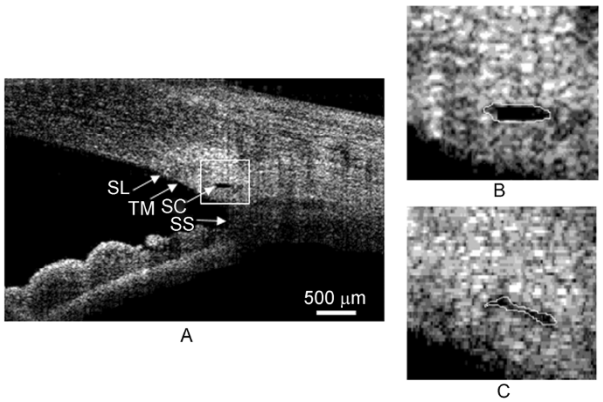


**Figure 2** The cross-sectional images from SS-OCT. A, The SS-OCT image of the anterior segment in a treated eye. B, The 4× image of a rectangular region in (A). C, The 4× image from an untreated eye. SC, Schlemm's canal; SL, Schwalbe's line; TM, trabecular mesh; SS, scleral spur.

## 2 Results

While in the supine, all participants were examined, by a single examiner. The anterior segment angle scan protocol was used for scanning the angle at the 3 and 9 o'clock positions, and each image contained 800 A-lines. Each position was imaged twice, and the images were stored for further analysis.

The morphometric SC values were measured and described as oculus dexter nasal (ODN), oculus dexter temporal (ODT), oculus sinister nasal (OSN) and oculus sinister temporal (OST). The anterior chamber angles of all 74 eyes were imaged, and the cross-sectional images showed the cornea, iris, scleral spur, trabecular meshwork and the SC. The values for the subjects including the long diameter, circumference, and area of the SC in treated and untreated eyes are shown in Figure 3. Five eyes could not be imaged, including two untreated eyes and three treated eyes. The success rate of imaging the SC was approximately 86.5% (in 128 of the 148 scans).

Statistical results were analyzed using Origin 19.0 (SPSS, IBM Inc., Chicago, Illinois, USA) to determine possible difference between the treated and untreated groups. A $P$-value less than 0.05 was considered statistically significant. The normal distribution was expressed as mean± standard deviation (SD).

The statistical values of long diameters, circumferences, and cross-section areas of the SCs in treated and untreated eyes are shown in Table 2. Date shown in Figure 3 demonstrated that the untreated group had the smallest morphometric values, particularly in the area of the SC. The corresponding statistical analysis demonstrated that the long diameters, circumferences, and areas of SCs in the treated group were larger than those in the untreated group, and the differences between the two groups were significant ($P_{\text{long diameter}}$<0.001; $P_{\text{circumference}}$<0.001; $P_{\text{area}}$<0.001).

**Table 2** Statistical results of SC morphometric values

| | | Mean | SD |
|---|---|---|---|
| Treated | Long diameter (μm) | 272.87806 | 25.7254 |
| | Circumference (μm) | 580.37891 | 44.96529 |
| | Cross-section area (μm$^2$) | 7935.6875 | 680.0036 |
| Untreated | Long diameter (μm) | 185.24047 | 19.72786 |
| | Circumference (μm) | 381.9026 | 41.22123 |
| | Cross-section area (μm$^2$) | 3890.71875 | 871.49844 |
| $P$-value | $P_{\text{long diameter}}$<0.001 | $P_{\text{circumference}}$<0.001 | $P_{\text{area}}$<0.001 |

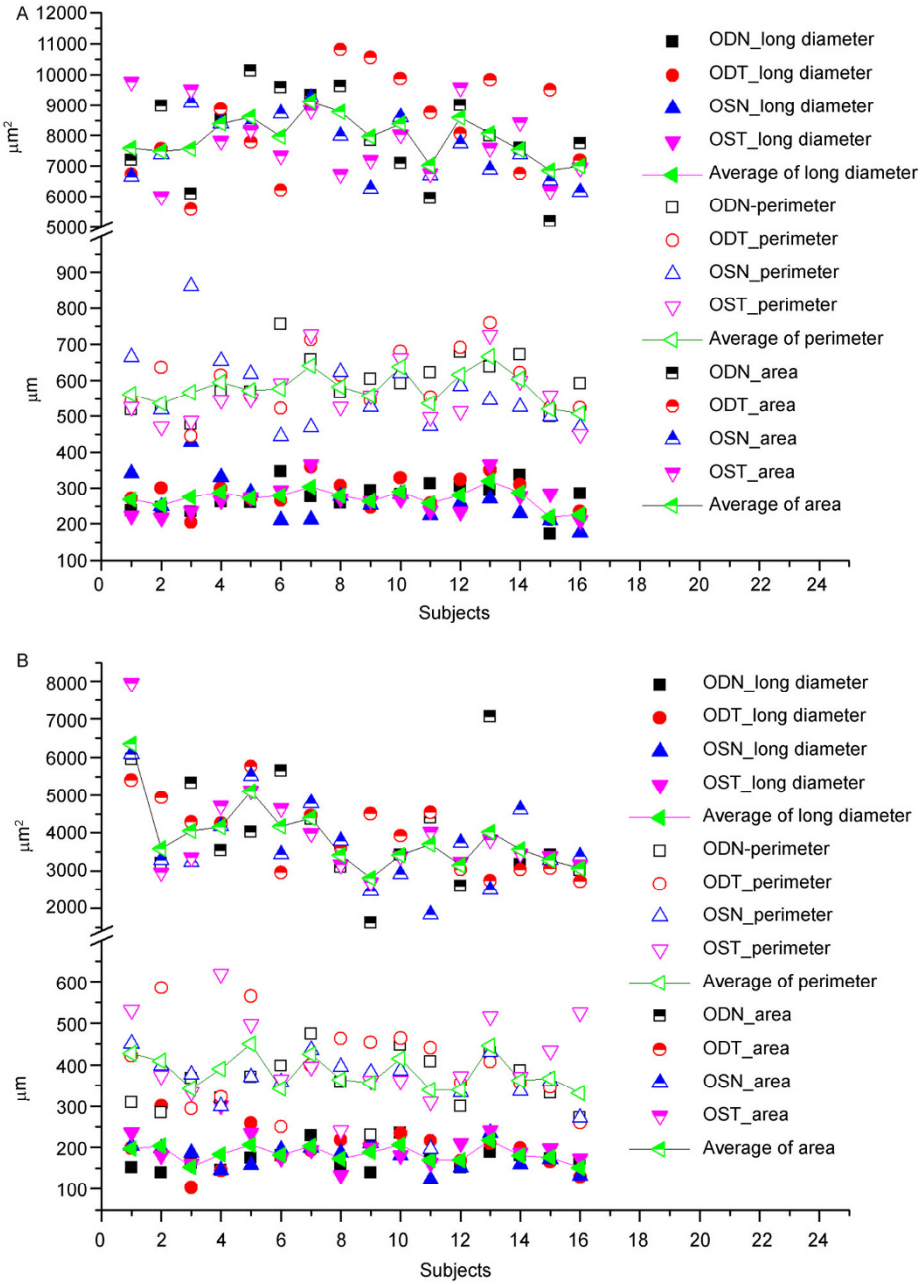


**Figure 3** The biological parameters of SCs in treated and untreated subjects. A, The distribution of the treated group. B, The distribution of the untreated group. The "average" means the average value of the OD and OS parameters, including the temporal and the nasal sides.

## 3 Discussion

High IOP is considered to be the most important risk factor for development of POAG, and its reduction continues to be the only successful way of treating the disease. The SC morphology is related to the aqueous outflow facility which regulates the IOP. Therefore, the change in SC morphology may be another parameter to assess the effects of drug treatment.

The objective of this study was to determine whether the SC morphometric values were changed with drug treatment. By using SS-OCT, the anterior chamber angle was imaged at high resolution, and SC could be recognized in these OCT imaging. The successful imaging rate was about 86.5% in a living human eye. The biological morphometric parameters of SC could be assessed properly, but because of subject movement from breathing and from eye movement, it was impossible to maintain the scanning plane (B-scan) perpendicular to the SC orientation in a living human eye. In the future, we will add a pupil camera to the SS-OCT system and improve the imaging speed to obtain real time three-dimensional image of SCs.

Three commonly used drugs, timolol, latanoprost, and

dorzolamide, have been used to treat POAG patients. Timolol and latanoprost reduced the production of aqueous humor, and dorzolamide improved the outflow of the aqueous humor. Though these drugs have different effects, the comparison experiments of drug treatments showed that these drugs could decrease the IOP [12,13].

Although the exact mechanism of POAG is still unclear, the statistical analysis showed that the area, circumference, and long diameter of the SC were smaller in untreated patients than in the treated patients. The data suggested that the SC became wider with low IOP, and collapsed when the IOP increased [5]. As Table 2 shows, after drug treatment, the mean cross-sectional area more than doubled. Thus, it is reasonable to deduce that, after drug therapy, the IOP would be reduced, which would lead to the expansion of the SC, causing the area and circumference to become larger. The larger SC may increase the aqueous drainage in POAG patients and could lead to a further reduction of IOP.

The use of OCT provides a non-invasive and new procedure in POAG pathogenesis research, which could facilitate the discovery of more effective and suitable methods to treat this disease. The statistical results obtained by the SS-OCT demonstrated that SC area may be an important index for POAG drug treatment efficacy. Although the size of the SC cannot be a criterion of POAG, it could provide a method to determine morphological changes in the SC with drug treatment. In our studies, widely used ocular hypotensive drugs including timolol, latanoprost, and dorzolamide were used to treat POAG patients. These three drugs have different mechanisms of action. Currently, the ethics approval of this research allowed us only to measure the morphological alterations of the glaucomatous human SC. Drug efficacy studies were therefore not done. The study was also limited by its small sample size, which is insufficient for a study of the effects of different treatment. In the future, we will recruit lager patient pool to investigate the effects of different treatment.

## 4 Conclusion

We found that the SC can be non-invasively imaged and measured in the living human eye by use of SS-OCT. The morphometric measurements of SCs were successfully performed, showing that after drug treatment, patients had larger SC morphometric values. This could explain the IOP reduction in the control eyes. These studies provide another perspective for *in vivo* glaucoma research. In the future, we hope to analyze correlations between the IOP and SC morphometric values in a larger group of eyes treated with different drugs.

*This work was supported by the Sichuan Youth Science & Technology Foundation (2013JQ0028), the National Natural Science Foundation of China (61108082), the West Light Foundation of the Chinese Academy of Sciences, and the National Major Scientific Equipment Program (2012YQ120080).*

1 Weinreb RN, Khaw PT. Primary open-angle glaucoma. Lancet, 2004, 363: 1711–1720
2 Sommer A, Tielsch JM, Katz J, Quigley HA, Gottsch JD, Javitt J, Singh K. Relationship between intraocular pressure and primary open angle glaucoma among white and black Americans. The Baltimore Eye Survey. Arch Ophthalmol, 1991, 109: 1090–1095
3 Bellezza AJ, Rintalan CJ, Thompson HW, Downs JC, Hart RT, Burgoyne CF. Deformation of the lamina cribrosa and anterior scleral canal wall in early experimental glaucoma. Invest Ophthalmol Vis Sci, 2003, 44: 623–637
4 Allingham RR, de Kater AW, Ethier CR. Schlemm's canal and primary open angle glaucoma: correlation between Schlemm's canal dimensions and outflow facility. Exp Eye Res, 1996, 62: 101–109
5 Hulzen RD, Johnsonl DH. Effect of fixation pressure on juxtacanalicular tissue and Schlemm's canal. Invest Ophthalmol Vis Sci, 1996, 37: 114–124
6 Nesterov AP. Role of the blockade of Schlemm's canal in pathogenesis of primary open-angle glaucoma. Am J Ophthalmol, 1970, 70: 691–696
7 Kagemann L, Wollstein G, Ishikawa H, Bilonick RA, Brennen PM, Folio LS, Gabriele ML, Schuman JS. Identification and assessment of Schlemm's canal by spectral domain optical coherence tomography. Invest Ophthalmol Vis Sci, 2010, 51: 4054–4059
8 Shi GH, Wang F, Li XQ, Lu J, Ding ZH, Sun XH, Jiang CH, Zhang YD. Morphometric measurement of Schlemm's canal in normal human eye using anterior segment swept source optical coherence tomography. J Biomed Opt, 2012, 17: 016016
9 Wang F, Shi GH, Li XQ, Lu J, Ding ZH, Sun XH, Jiang CH, Zhang YD. Comparison of Schlemm's canal's biological parameters in primary open-angle glaucoma and normal human eyes with swept source optical coherence tomography. J Biomed Opt, 2012, 17: 116008
10 Shi GH, Wang F, Li XQ, Lu J, Sun XH, Jiang CH, Zhang YD. Assessment of Schlemm's canal in a normal human eye by swept source optical coherence tomography. Laser Phys Lett, 2013, 10: 075602
11 Orzalesi N, Rossetti L, Invernizzi T, Bottoli A, Autelitano A. Effect of timolol, latanoprost, and dorzolamide on circadian IOP in glaucoma or ocular hypertension. Invest Ophthalmol Vis Sci, 2000, 41: 2566–2573
12 Quaranta L, Gandolfo F, Turano R, Rovida F, Pizzolante T, Musig A, Gandolfo E. Effects of topical hypotensive drugs on circadian IOP, blood pressure, and calculated diastolic ocular perfusion pressure in patients with glaucoma. Invest Ophthalmol Vis Sci, 2006, 47: 2917–2923
13 Li P, Reif R, Zhi ZW, An L, Martin E, Shen T, Johnstone M, Wang RK. Phase-sensitive optical coherence tomography characterization of pulse-induced trabecular meshwork displacement in *ex vivo* non-human primate eyes. J Biomed Opt, 2012, 17: 076026
14 Li XQ, Shi GH, Zhang YD. Time domain interpolation on graphics processing unit. J Innovat Opt Health Sci, 2011, 4: 89–95